

Generation of intense cylindrical vector beams by Faraday effect in plasma

Wei Liu,¹ Qing Jia,^{1,*} and Jian Zheng^{1,2}

¹*Department of Plasma Physics and Fusion Engineering,*

University of Science and Technology of China, Hefei, Anhui 230026, People's Republic of China

²*Collaborative Innovation Center of IFSA, Shanghai Jiao Tong University, Shanghai 200240, People's Republic of China*

(Dated: July 4, 2023)

Cylindrical vector (CV) beams, whose polarizations are cylindrically symmetric, have recently been widely applied in high energy density physics such as electron acceleration and intense spatiotemporal optical vortices generation. Thermal-damage-resistant plasma optics are expected to generate intense CV beams. In this work, based on the Faraday effect, we propose a method that can directly convert an intense linearly/circularly polarized Gaussian beam into a CV/vortex beam by setting up an azimuthally distributed axial magnetic field in the plasma. Three-dimensional particle-in-cell simulations demonstrate good conversion efficiency, which offers a new degree of freedom for manipulating high-power laser pulses and paves the way for further studies on ultra-strong vector beams. In addition, our work reveals a new possible source of photon orbital angular momentum related to magnetized plasma in astrophysics and space physics.

Polarization is one of the fundamental properties of electromagnetic wave. In laser plasma physics, there are many processes that are closely related to laser polarization, such as laser resonance absorption[1, 2], axial self-generated magnetic field[3, 4], high harmonic generation[5–8] and electron acceleration[9]. In these works, electromagnetic waves are typically considered linearly or circularly polarized, whose polarizations are uniformly distributed in the transverse plane. Exotic laser beams with transversely non-uniformly distributed polarization, namely, vector beams[10], have attracted much attention in the past two decades. Cylindrical vector (CV) beams[11] are a special class of vector beams whose polarizations are cylindrically distributed. Representative radially polarized (RP) and azimuthally polarized (AP) electromagnetic waves have been studied extensively mainly due to their unique focusing characteristics[12, 13]. It has been proven that RP beam can be focused more tightly than linearly polarized beam. Near the focal plane, the tightly focused RP(AP) beam will result in strong longitudinal electric (magnetic) fields near the optical axis.

Weak CV beams have been employed in fields such as super-resolution imaging[14] and optical trapping[15]. Recently, intense CV beams have been of interest in laser plasma physics and have brought some new effects. Due to the strong longitudinal electric fields, RP beam is applied in the direct laser acceleration of electrons[16, 17]. In particular, when using a plasma mirror as an electron injector, electron bunches with MeV energies and hundreds of pC charges are obtained[17]. In addition, it demonstrates that intense spatiotemporal optical vortices[18, 19] can be generated by intense RP beams obliquely reflected from a solid-plasma surface[20].

However, as far as we know, the generation of intense CV beams remains challenging. Conventional methods

for generating intense CV beams[21–23] might be restricted due to the optical thermal threshold. Plasma, benefiting from sustaining very high light intensity, has recently been widely used to manipulate intense lights, such as plasma mirrors to improve the temporal contrast of femtosecond pulses[24], plasma-based options to generate vortex beam[25–29], holographic plasma lenses to focus intense lasers[30], plasma photonic crystals[31] and so on. In this study, utilizing the Faraday effect[32], we propose a straightforward and effective plasma-based approach for converting an intense linearly/circularly polarized Gaussian beam into a CV/vortex beam.

The investigation of plasma-based generation of vector beam and vortex beam in the laboratory also holds significant importance for observations in astrophysics and space physics. Currently, our understanding of the universe is primarily derived from observations of electromagnetic waves. It is crucial to extract as much information as possible from the collected electromagnetic waves, given the scarcity of data and the high cost. Recently, the photon orbital angular momentum (POAM)[33], which is linked to the vortex beam, is increasingly attracting attention as a new degree of freedom in the field of astronomy[34–38]. In 2003, Harwit outlined several potential sources of astrophysical POAM[34] from radiation emitted by luminous pulsars and quasars to the cosmic microwave background radiation. Especially, a recent study[37] has confirmed the presence of POAM generated by the gravitational effect near rotating black holes, as previously proposed by Tamburini *et al.* [36]. And this research demonstrates that POAM can be directly employed to measure the rotation parameters of a black hole. It is worth noting that plasmas found in the universe and celestial bodies are often magnetized, such as the plasmas in magnetic reconnection process[39]. We are curious whether POAM can be generated after electromagnetic waves passing through these magnetized plasmas and whether they can be used for relevant observations.

The difference in dispersion between left- and right-

* qjia@ustc.edu.cn

hand circularly polarized electromagnetic waves in axially magnetized plasma is a well-established phenomenon that gives rise to distinct phase and group velocities[40]. Taking into account the difference in *group velocity*, simulations have shown that a linearly polarized laser pulse passing through an axially magnetized plasma can split into two laser pulses with opposite circular polarizations, provided the axial magnetic field is strong enough[41]. Considering the differences in *phase velocities*, the polarization of a linearly polarized laser undergoes rotation after passing through an axially magnetized plasma, which is referred to as the Faraday effect[40]. We will now provide a brief overview of the Faraday effect and offer a brief introduction to the generation of CV beam based on it.

The propagation of left- and right-hand circularly polarized electromagnetic waves along a weakly magnetic field ($|\omega_{ce}/\omega| \ll 1$) in a plasma is associated with different dispersions, which can be expressed[40]

$$N_{L/R} = \frac{kc}{\omega} \approx \sqrt{1 - \frac{n_e}{n_c}} \pm \frac{1}{2} \frac{1}{\sqrt{1 - \frac{n_e}{n_c}}} \frac{n_e \omega_{ce}}{n_c \omega}, \quad (1)$$

where $N_{L/R}$ is the refractive index for left/right-hand circularly polarized electromagnetic wave, k is the laser wavenumber in magnetized plasma, c is the speed of light in vacuum, ω is the laser frequency, n_e is the electron number density, $n_c = \varepsilon_0 m_e \omega^2 / e^2$ is the critical number density, m_e is the electron mass, $\omega_{ce} = eB_x / m_e$ is the electron cyclotron frequency, e is the elementary charge, and B_x is the axial magnetic field.

The incident linearly polarized electromagnetic wave can be represented as $\mathbf{E}_{in} = [(\mathbf{e}_y - i\mathbf{e}_z) + (\mathbf{e}_y + i\mathbf{e}_z)]E_0 \exp[i(k_0x - \omega t)]$, where $\sigma_x = \pm 1$ in $\mathbf{e}_y + \sigma_x i\mathbf{e}_z$ represent right/left-hand circularly polarized and k_0 is the laser wavenumber in vacuum. After propagating distance L , the output wave can be written as

$$\mathbf{E}_{out} = 2E_0(\cos \varphi \mathbf{e}_y + \sin \varphi \mathbf{e}_z) \exp(i\Phi - i\omega t), \quad (2)$$

where $\varphi = k_0L(N_L - N_R)/2$, $\Phi = k_0L(N_L + N_R)/2 = k_0L\sqrt{1 - n_e/n_c}$. The output wave is still linearly polarized but with polarization rotation angle

$$\varphi \approx \frac{1}{2} \frac{1}{\sqrt{1 - \frac{n_e}{n_c}}} \frac{n_e \omega_{ce}}{n_c \omega} k_0L. \quad (3)$$

The Faraday rotation angle is directly linked to plasma density, plasma length, and the strength of the axial magnetic field. In most cases, researchers focus on studying a plasma with uniform magnetization in the transverse plane, which ensures that the output beam remains linearly polarized. However, this uniformity restricts the degree of polarization manipulation that can be achieved. In cases where the magnetization in the transverse plane is non-uniform, the incident linearly polarized beam undergoes a transformation into a vector beam. By skillfully designing the distribution of the magnetic field, it

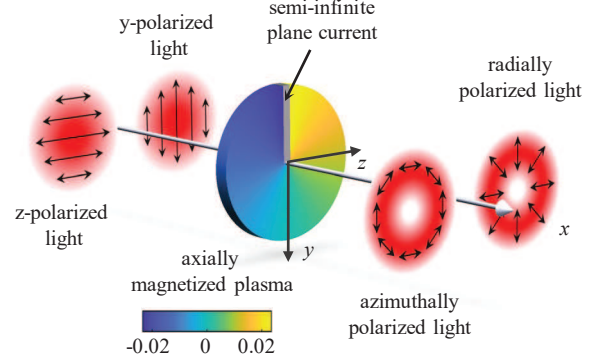


FIG. 1. Illustration of a linearly y/z-polarized beam transformed into a RP/AP beam after passing through an axially (x) magnetized plasma (normalized by $m_e\omega/e$).

becomes possible to generate a vector beam with desired characteristics, such as a CV beam.

The simplified distribution of a RP beam at the waist can be written as[11]

$$\mathbf{E} = E_0 \left(\frac{r}{w_0} \right) \exp \left(-\frac{r^2}{w_0^2} \right) \exp[i(k_0x - \omega t)] \mathbf{e}_r, \quad (4)$$

where w_0 is the beam waist, $r = \sqrt{y^2 + z^2}$ and $\theta = \arctan(z/y)$. A significant difference between a RP beam and a linearly polarized beam is that the polarization of a RP beam varies across different spatial locations, but all along the radial direction. In order to convert linearly polarized beam into RP beam, it is necessary to introduce spatially varying Faraday rotation angles $\varphi(\theta)$. We have discovered that by setting the Faraday rotation angle in Eq. (3) as $\varphi(r, \theta) = \theta$, the incident laser beam with linear polarization in the y direction can be converted into RP beam, as illustrated in Fig. 1. By altering the polarization direction of the incident beam, other CV beams like AP beam can be obtained in principle.

Furthermore, in accordance with Eq. (2), the Faraday rotation not only induces the rotation of laser polarization but also introduces an additional phase Φ . In order to prevent the introduction of a spiral phase $\exp(i\theta)$ for CV beams[11], the phase Φ should be independent of azimuth, which implies that $\varphi(r, \theta) = \theta$ can be achieved by setting an azimuthally distributed axial magnetic field $B_x = B_{ext}\theta$ with

$$B_{ext} = \frac{2m_e\omega n_c \sqrt{1 - \frac{n_e}{n_c}}}{en_e k_0L}. \quad (5)$$

This magnetic field distribution, depicted in Fig. 1, can be generated approximately by a semi-infinite plane current. Further details and a comprehensive discussion on this topic will be provided in Sec. ??.

To verify the above scheme, three-dimensional (3D) particle-in-cell (PIC) simulations are conducted with the code Smilei[42]. A linearly polarized Gaussian beam with wavelength $\lambda = 1\mu\text{m}$ (in vacuum) and radius of waist $w_0 = 10\mu\text{m}$ normally incidents on a plasma located at $15\mu\text{m} < x < 65\mu\text{m}$. The laser intensity rises linearly over 10 laser periods to its maximum intensity $I_0 = 1.37 \times 10^{14}\text{W}/\text{cm}^2$ (corresponding to $a_0 = eE_0/m_e\omega c = 0.01$) and then remains constant. The simulation box is $80\mu\text{m}(x) \times 50\mu\text{m}(y) \times 50\mu\text{m}(z)$ with $1280 \times 400 \times 400$ cells. The cell sizes are $dx = \lambda/16$, $dy = dz = \lambda/8$. Each cell has applied 16 particles for electrons, and the ions are set to be immobile. The electrons are uniformly distributed with number density $n_e = 6.27 \times 10^{26}\text{m}^{-3}$, corresponding to $0.56n_c$. The axial magnetic field distribution is set as Eq. (5) with $B_{ext}=80.17\text{T}$, which satisfies $|\omega_{ce}/\omega| \ll 1$. It should be noted that in the simulations, such magnetic field only participates in pushing the particles but does not participate in the Maxwell solver[42], which can be regarded as the steady magnetic field generated by an external current or kinds of magnets and is physically reasonable.

Figure 2 presents the laser amplitude and electric field vector distributions when lasers exiting the magnetized plasma for different linearly polarized incident Gaussian beams. Figure 2(a) displays the result of a y-polarized Gaussian beam passing through the plasma. The laser intensity is modulated to have a null intensity in the center, which is a key feature of the CV beam. Besides, judging from the distribution of the laser electric field vectors represented by the small white arrows, the linearly polarized beam is successfully converted into a RP beam. Similarly, the result of the transformation of a z-polarized Gaussian beam into an AP beam is shown in

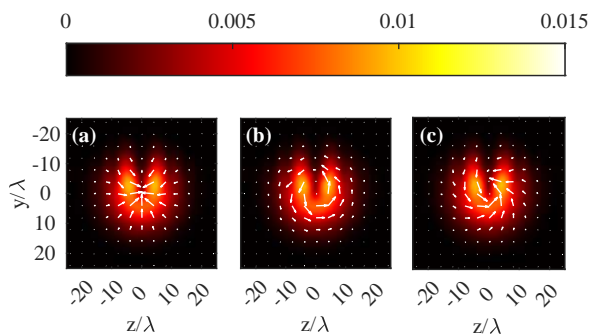


FIG. 2. PIC simulation results of laser amplitude (normalized by $m_e\omega c/e$) and electric field vector distributions after different linearly polarized beams pass through the $B_x = B_{ext}\theta$ magnetized plasma at $x = 65\mu\text{m}$. (a) RP beam generated by a y-polarized Gaussian beam; (b) AP beam generated by a z-polarized Gaussian beam; (c) A generalized CV beam generated by linear superposition of y-polarized and z-polarized Gaussian beams. The background color scale shows the laser amplitude, and the white arrows represent the electric field vectors.

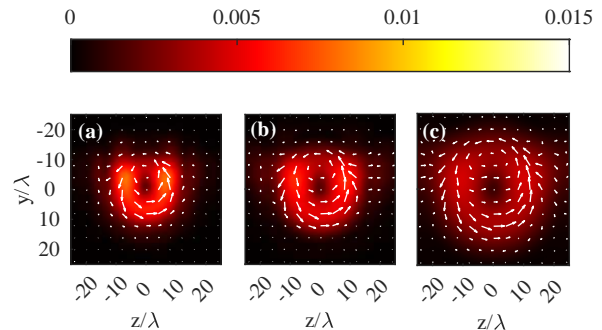


FIG. 3. Distributions of electric field vectors and laser amplitude (normalized by $m_e\omega c/e$) as the RP beam leaves the plasma and propagates at different distances in vacuum: (a) $\Delta x = 50\mu\text{m}$, (b) $\Delta x = 100\mu\text{m}$, (c) $\Delta x = 200\mu\text{m}$. The distance Δx is referenced by $x = 65\mu\text{m}$, where the laser exits the plasma. These results are calculated from the electric field given by the PIC simulation through the angular spectrum method. The background color scale shows the laser amplitude, and the white arrows represent the electric field vectors.

Fig. 2(b). In general, an arbitrary CV beam can be generated by a reasonable linear superposition of y-polarized and z-polarized Gaussian beams, as indicated in Fig. 2(c).

Note that in Fig. 2, the intensity of the laser is significantly modulated near the line of $z = 0$ ($y < 0$). In our theoretical scheme, the axial magnetized plasma is regarded as an optical medium with the dispersion relation shown in Eq. (1), which requires the scale length of the electron motion ($L_{ele} \propto a_0\lambda$ when $a_0 < 1$) to be much smaller than the scale length of the magnetic field ($L_{mag} \sim |rB_x/(\partial B_x/\partial\theta)|$). This condition is satisfied in most areas except the region near the line of $z = 0$ ($y < 0$), where a large gradient in the magnetic field exists as revealed in Fig. 1. This large magnetic gradient leads to non-typical motions of electrons, which significantly modulates the laser intensity as shown in the PIC simulations. However, these mode imperfections will gradually decrease as the laser exits the plasma and propagates in vacuum.

Figures 3(a)-(c) present the distributions of electric field vectors and amplitude when the generated RP beam exits the plasma and propagates in vacuum after $50\mu\text{m}$, $100\mu\text{m}$ and $200\mu\text{m}$, respectively. These results are calculated from the electric field given by the PIC simulation corresponding to Fig. 2(b) through the angular spectrum method[43]. In comparison with Fig. 2(b), it hints that the intensity modulation initially near the line of $z = 0$ ($y < 0$) gradually decreases. This may be due to the stronger diffraction of the above higher-order-mode imperfections compared with the main component of the RP beam. These results further illustrate the practicality of our scheme in generating CV beams.

The above magnetized plasma can also be utilized for the generation of vortex beam[25–29]. When the incident

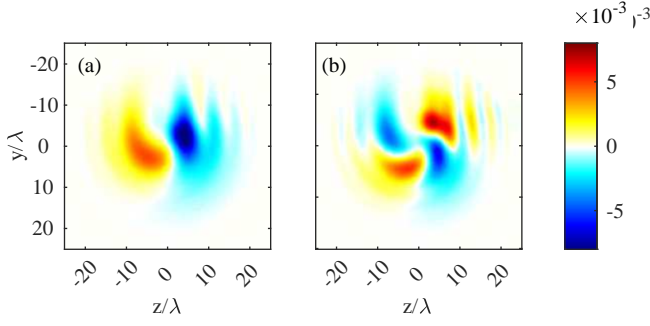


FIG. 4. Distributions of electric field E_z (normalized by $m_e \omega c / e$) after right-hand circularly polarized ($\sigma_x = 1$) Gaussian beams pass through different magnetized plasmas with (a) $\eta = 1$, (b) $\eta = 2$. Other parameters are the same with those in Fig. 2.

beam is circularly polarized, according to Eq. (1), the laser exiting from the $B_x = B_{ext}\theta$ magnetized plasma can be written as

$$\mathbf{E}_{out} = (\mathbf{e}_y + \sigma_x i \mathbf{e}_z) E_0 e^{i(k_0 L \sqrt{1 - \frac{n_e}{n_c}} - \omega t - \eta \sigma_x \theta)}, \quad (6)$$

where $\eta = ek_0 L n_e B_{ext} / (2m_e \omega n_c \sqrt{1 - n_e/n_c})$. The output beam is still circularly polarized but with a spiral phase $\exp(-i\eta \sigma_x \theta)$, which indicates that the exiting laser has been converted into a vortex beam with azimuthal index $l = -\eta \sigma_x$ [33].

Figure 4(a) presents the electric field E_z distribution obtained by PIC simulation when a right-hand circularly polarized ($\sigma_x = 1$) laser exits the above magnetized plasma ($\eta = 1$). The two-flap distribution indicates that the existing laser is mainly dominated by the vortex mode with $|l| = 1$. By performing the Laguerre-Gaussian (LG) mode decomposition [25], the output laser can be predominantly described as $\sqrt{0.04} e^{2.28i} LG_{0,0} + \sqrt{0.66} e^{1.41i} LG_{0,-1} + \sqrt{0.09} e^{0.77i} LG_{1,-1}$. Here, $\sqrt{a_{p,l}} e^{i\phi} LG_{p,l}$ refers to the LG mode with an azimuthal index l and a radial index p . It is noteworthy that the waist radius of the LG modes is selected to match that of the incident Gaussian mode. This mode decomposition highlights that an incident Gaussian beam can be effectively converted into a vortex beam with topological charge of $l = -1$. Increasing the parameter η allows for the generation of vortex beams with higher values of $|l|$. Figure 4(b) displays the distribution of the electric field E_z when a right-hand circularly polarized ($\sigma_x = 1$) beam exits the magnetized plasma with $\eta = 2$. By making the mode decomposition, it is found that the existing laser is dominated by the LG mode with $l = -2$.

In the above PIC simulations, a relatively strong magnetic field $B_{ext} \approx 80$ T and high plasma density $n_e = 6.27 \times 10^{26} \text{ m}^{-3}$ are applied to reduce the simulation cost. Indeed, the requirement of the strength of the magnetic field and plasma density can be significantly reduced. Figure 5 shows the dependence of the normalized plasma

length L/λ on the normalized plasma density n_e/n_c and the strength of the normalized magnetic field B_{ext}/B_0 . This indicates that a longer plasma length is beneficial for reducing the magnetic field strength as well as the plasma density. For lasers with $\lambda = 1 \mu\text{m}$, if the plasma length is chosen as $L = 2$ cm and the plasma density is $n_e = 4.46 \times 10^{25} \text{ m}^{-3}$, the required magnetic field is only approximately 4 T and is easily achieved experimentally.

In our approach, the generation of an axial magnetic field with $B_x = B_{ext}\theta$ is a crucial aspect. We consider a magnetic field that solely possesses an axial component B_x , without any azimuthal (B_θ) or radial (B_r) components. It can be readily verified that this magnetic field satisfies the divergence equation $\nabla \cdot \mathbf{B} = 0$. To fulfill the curl equation $\nabla \times \mathbf{B} = \mu_0 \mathbf{J}$, it is necessary to introduce a current $\mathbf{J} = B_{ext} \sum_{n=1}^{\infty} n a_n \cos(n\theta) / (\mu_0 r) \mathbf{e}_r$, where $a_n = \int_{-\pi}^{\pi} \theta \sin(n\theta) d\theta / \pi = -2(-1)^n / n$. This current can be regarded as the source term responsible for the generation of the $B_x = B_{ext}\theta$ axial magnetic field.

Figure 6(a) displays the distribution of this current (in radial direction) when n is taken until 40. It indicates that this current is mainly distributed near the line of $z = 0$ ($y < 0$). However, it is worth noting that the current tends to approach infinity as r approaches 0, making it practically impossible to obtain experimentally. To overcome this limitation, we propose employing a semi-infinite flat plate current that addresses the characteristics of the current. This current can be represented as

$$J_y / J_0 = \frac{\pi \lambda B_{ext}}{B_0 L_z \cosh^2(z/L_z) [1 + \exp(y/\lambda)]}, \quad (7)$$

where $J_0 = n_c e c$, $B_0 = m_e \omega / e$, L_z denotes the characteristic thickness of this current in z direction. The distribution of this current when $L_z = \lambda$ is presented in

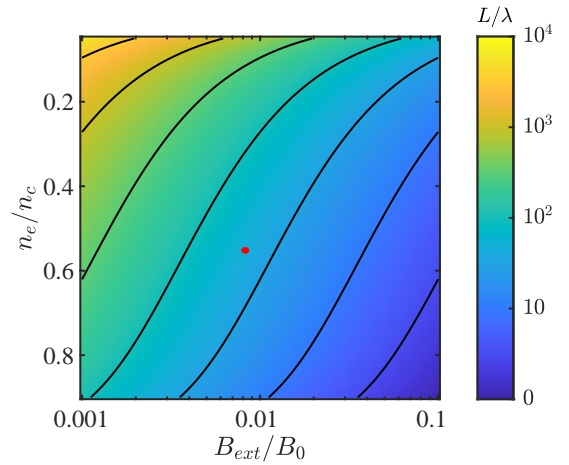


FIG. 5. Contour plot of the plasma length L (normalized by λ) with different plasma densities n_e (normalized by n_c) and strengths of the axial magnetic field B_{ext} (normalized by $B_0 = m_e \omega / e$). The red point represents the parameters used in the above PIC simulations.

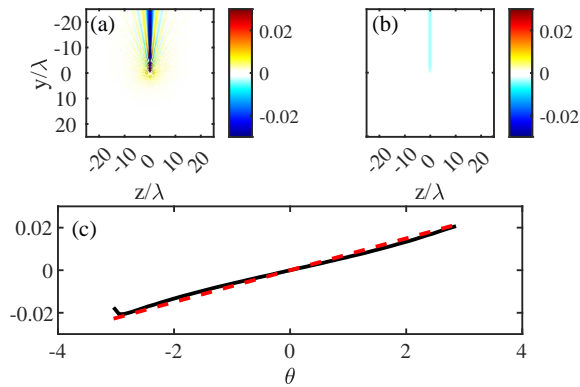


FIG. 6. (a) Distribution of current J_r/J_0 obtained by theoretical calculation; (b) Distribution of a semi-infinite plane current J_r/J_0 ($\approx -J_y/J_0$); (c) Comparison of magnetic fields (normalized by $m_e\omega/e$) generated by the semi-infinite plane current (black solid line) and theoretical magnetic field (red dashed line) at $r = w_0 = 10\lambda$.

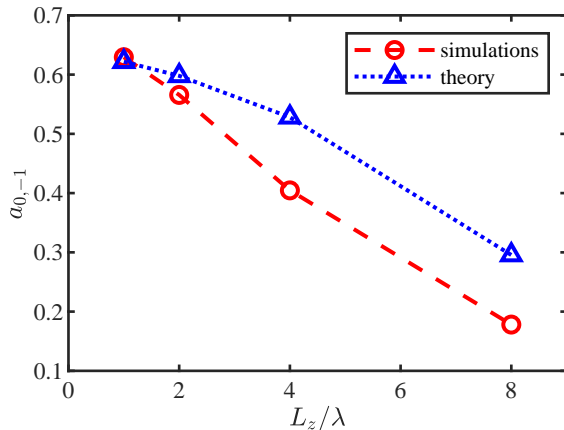


FIG. 7. The variation of the $LG_{0,-1}$ mode energy occupancy ratio ($a_{0,-1}$) of the outgoing beam with respect to the current sheet thickness (L_z). The data represented by red circles is obtained from PIC simulations, while by blue upward-pointing triangles is provided by a simplified theory.

Fig. 6(b). Figure 6(c) compares the magnetic field generated by this planar current at $r = 10\lambda$ with the magnetic field $B_x = B_{ext}\theta$. It is evident that the two magnetic field lines overlap significantly. We employed this magnetic field into the PIC simulation to examine the transformation of a circularly polarized Gaussian beam into a vortex beam. By performing the LG decomposition on the output beam, we obtained $\sqrt{0.07}e^{1.81i}LG_{0,0} + \sqrt{0.63}e^{1.34i}LG_{0,-1} + \sqrt{0.08}e^{0.7i}LG_{1,-1}$, which are nearly identical to those obtained previously.

It is worth noting the similarity between the current described in Eq. (7) and the Harris current in the magnetic reconnection process[39, 44], especially in cases involving with the spatially confined X-line in the current

direction[45, 46]. This resemblance implies that the passage of an electromagnetic wave through a magnetic reconnection region can potentially result in the generation of POAM and carry important information along its path. Considering the magnetic reconnection in solar flares, typical parameters are magnetic field strength $B_{ext} \sim 0.01$ T, plasma density $n_e \sim 3 \times 10^{15} \text{ m}^{-3}$ and plasma length $L \sim 10^8 \text{ m}$ [47]. According to Eq. (5), for electromagnetic waves with wavelengths greater than $20 \mu\text{m}$, it is possible to be detected as carrying POAM. This result can be confirmed in principle. In addition, the magnetic reconnection in solar flares can now be studied in the laboratory[48] based on the scaling laws[49]. Commonly used parameters in the investigation of magnetic field reconnection based on laser plasma processes are $B_{ext} \sim 100$ T and $n_e \sim 5 \times 10^{25} \text{ m}^{-3}$. For laser with $\lambda = 800 \text{ nm}$, the plasma length required to produce significant POAM is about 1 mm, which is experimentally achievable.

The POAM carried by the outgoing electromagnetic waves holds potential for diagnosing and observing relevant physical quantities. In the case of magnetic reconnection with a spatially confined X-line extent[45, 46], the magnetic fields at the two ends of the current sheet undergo opposite azimuthal changes, leading to the generation of opposing POAMs. This property can be employed for the diagnosis of the length of X-line. Furthermore, the thickness of the current sheet is a significant aspect in the investigation of magnetic reconnection. We conducted a simple study on the conversion of circularly polarized beam passing through magnetized plasma with varying current sheet thicknesses L_z . Figure 7 displays the dependence of $LG_{0,-1}$ mode energy occupancy $a_{0,-1}$ on L_z , as determined through PIC simulations and a simplified theory. In the PIC simulations, the parameters remain consistent with the previous setup, except for adjusting the current sheet thickness L_z . The simplified theory results are obtained by directly incorporating the phase induced by the magnetized plasma into the incident Gaussian beam, followed by the LG mode decomposition. It is evident that the percentage of $LG_{0,-1}$ decreases as L_z increases. These findings suggest the potential use of POAM in diagnosing[35, 50] the thickness of the current sheet. However, it must be noted that the results are also influenced by the plasma length and the beam waist of the incident beam, which require further investigation.

Besides the magnetic reconnection process, there are other physical processes or objects in the universe that have magnetic fields near them. For example, the magnetic field near a magnetar can be as strong as 10^8 T, and whether POAM can be obtained when electromagnetic waves pass through this region is worth further investigation.

In conclusion, a scheme converting the incident intense linearly polarized Gaussian beam into a cylindrical vector beam is proposed, which is achieved by setting up an axial magnetic field with azimuthal distribution

$B_x = B_{ext}\theta$. Three-dimensional particle-in-cell simulation results verify the feasibility and efficiency of this scheme. Besides, when considering circularly polarized Gaussian beam passing through the proposed magnetized plasma, vortex beam with $|l| = 1$ can be generated. By increasing the strength of the magnetic field B_{ext} (or plasma length L , electron number density n_e), arbitrarily higher $|l|$ mode vortex beams can also be generated. This scheme is free of the optical thermal threshold and is applicable for intense lasers with powers as high as \sim PW in some laser facilities.

Our investigation also reveals a promising and novel source of photon orbital angular momentum in astrophysics and space physics. Specifically, we have demonstrated that orbital angular momentum can be acquired by an electromagnetic wave passing through a magnetic

reconnection region. This photon orbital angular momentum holds the potential for diagnosing the length of the X-line and the thickness of the current sheet in this process. Further research is required to explore and understand these possibilities in greater depth.

ACKNOWLEDGMENTS

This research was supported by the National Natural Science Foundation of China (NSFC) under Grant No. 11975014, by the Strategic Priority Research Program of Chinese Academy of Sciences, Grant Nos. XDA25050400 and XDA25010200. The authors would like to thank and acknowledge Q. Lu and K. Huang for helpful discussions.

-
- [1] J. P. Freidberg, R. W. Mitchell, R. L. Morse, and L. I. Rudinski, Resonant absorption of laser light by plasma targets, *Physical Review Letters* **28**, 795 (1972).
- [2] W. Woo, K. Estabrook, and J. S. DeGroot, Resonant absorption of laser light by a magnetized plasma, *Physical Review Letters* **40**, 1094 (1978).
- [3] J. Deschamps, M. Fitaire, and M. Lagoutte, Inverse faraday effect in a plasma, *Physical Review Letters* **25**, 1330 (1970).
- [4] M. G. Haines, Generation of an axial magnetic field from photon spin, *Physical Review Letters* **87**, 135005 (2001).
- [5] P. B. Corkum, Plasma perspective on strong field multiphoton ionization, *Physical Review Letters* **71**, 1994 (1993).
- [6] S. V. Bulanov, N. M. Naumova, and F. Pegoraro, Interaction of an ultrashort, relativistically strong laser pulse with an overdense plasma, *Physics of Plasmas* **1**, 745 (1994).
- [7] R. Lichters, J. Meyer-ter-Vehn, and A. Pukhov, Short-pulse laser harmonics from oscillating plasma surfaces driven at relativistic intensity, *Physics of Plasmas* **3**, 3425 (1996).
- [8] F. Quéré, C. Thauray, P. Monot, S. Dobosz, P. Martin, J. P. Geindre, and P. Audebert, Coherent wake emission of high-order harmonics from overdense plasmas, *Physical Review Letters* **96**, 125004 (2006).
- [9] B. Liu, H. Y. Wang, J. Liu, L. B. Fu, Y. J. Xu, X. Q. Yan, and X. T. He, Generating overcritical dense relativistic electron beams via self-matching resonance acceleration, *Physical Review Letters* **110**, 045002 (2013).
- [10] H. Rubinsztein-Dunlop, A. Forbes, M. V. Berry, M. R. Dennis, D. L. Andrews, M. Mansuripur, C. Denz, C. Alpmann, P. Banzer, T. Bauer, E. Karimi, L. Marrucci, M. Padgett, M. Ritsch-Marte, N. M. Litchinitser, N. P. Bigelow, C. Rosales-Guzmán, A. Belmonte, J. P. Torres, T. W. Neely, M. Baker, R. Gordon, A. B. Stilgoe, J. Romero, A. G. White, R. Fickler, A. E. Willner, G. Xie, B. McMorran, and A. M. Weiner, Roadmap on structured light, *Journal of Optics* **19**, 013001 (2016).
- [11] Q. Zhan, Cylindrical vector beams: from mathematical concepts to applications, *Advances in Optics and Photonics* **1**, 10.1364/aop.1.000001 (2009).
- [12] S. Quabis, R. Dorn, M. Eberler, O. Glöckl, and G. Leuchs, Focusing light to a tighter spot, *Optics Communications* **179**, 1 (2000).
- [13] R. Dorn, S. Quabis, and G. Leuchs, Sharper focus for a radially polarized light beam, *Phys Rev Lett* **91**, 233901 (2003).
- [14] Y. Kozawa, D. Matsunaga, and S. Sato, Superresolution imaging via superoscillation focusing of a radially polarized beam, *Optica* **5**, 86 (2018).
- [15] Q. Zhan, Trapping metallic rayleigh particles with radial polarization, *Optics Express* **12**, 3377 (2004).
- [16] N. Zaim, M. Thevenet, A. Lifschitz, and J. Faure, Relativistic acceleration of electrons injected by a plasma mirror into a radially polarized laser beam, *Phys Rev Lett* **119**, 094801 (2017).
- [17] N. Zaïm, D. Guénot, L. Chopineau, A. Denoeud, O. Lundh, H. Vincenti, F. Quéré, and J. Faure, Interaction of ultraintense radially-polarized laser pulses with plasma mirrors, *Physical Review X* **10**, 10.1103/PhysRevX.10.041064 (2020).
- [18] K. Y. Bliokh and F. Nori, Spatiotemporal vortex beams and angular momentum, *Phys. Rev. A* **86**, 033824 (2012).
- [19] A. Chong, C. Wan, J. Chen, and Q. Zhan, Generation of spatiotemporal optical vortices with controllable transverse orbital angular momentum, *Nature Photonics* **14**, 350 (2020).
- [20] Z.-Y. Chen, R. Hu, S. Zhang, and T. Yuan, Relativistic high-order harmonic generation of spatiotemporal optical vortices, *Physical Review A* **106**, 013516 (2022).
- [21] D. Pohl, Operation of a ruby laser in the purely transverse electric mode te_{01} , *Applied Physics Letters* **20**, 266 (1972).
- [22] G. Machavariani, Y. Lumer, I. Moshe, A. Meir, and S. Jackel, Spatially-variable retardation plate for efficient generation of radially- and azimuthally-polarized beams, *Optics Communications* **281**, 732 (2008).
- [23] S. Chen, X. Zhou, Y. Liu, X. Ling, H. Luo, and S. Wen, Generation of arbitrary cylindrical vector beams on the higher order poincaré sphere, *Optics Letters* **39**, 5274 (2014).
- [24] C. Thauray, F. Quéré, J. P. Geindre, A. Levy, T. Ceccotti,

- P. Monot, M. Bougeard, F. Réau, P. d'Oliveira, P. Audebert, R. Marjoribanks, and P. Martin, Plasma mirrors for ultrahigh-intensity optics, *Nature Physics* **3**, 424 (2007).
- [25] Y. Shi, B. Shen, L. Zhang, X. Zhang, W. Wang, and Z. Xu, Light fan driven by a relativistic laser pulse, *Physical Review Letters* **112**, 10.1103/physrevlett.112.235001 (2014).
- [26] J. Vieira, R. M. G. M. Trines, E. P. Alves, R. A. Fonseca, J. T. Mendonça, R. Bingham, P. Norreys, and L. O. Silva, Amplification and generation of ultra-intense twisted laser pulses via stimulated raman scattering, *Nature Communications* **7**, 10371 (2016).
- [27] A. Leblanc, A. Denoeud, L. Chopineau, G. Mennerat, P. Martin, and F. Quéré, Plasma holograms for ultrahigh-intensity optics, *Nature Physics* **13**, 440 (2017).
- [28] K. Qu, Q. Jia, and N. J. Fisch, Plasma q -plate for generation and manipulation of intense optical vortices, *Physical Review E* **96**, 053207 (2017).
- [29] T. Long, C. Zhou, L. Ju, T. Huang, M. Yu, K. Jiang, C. Wu, S. Wu, H. Zhang, B. Qiao, S. Ruan, and X. He, Generation of relativistic vortex laser beams by spiral shaped plasma, *Phys. Rev. Res.* **2**, 033145 (2020).
- [30] M. R. Edwards, V. R. Munirov, A. Singh, N. M. Fasano, E. Kur, N. Lemos, J. M. Mikhailova, J. S. Wurtele, and P. Michel, Holographic plasma lenses, *Phys Rev Lett* **128**, 065003 (2022).
- [31] G. Lehmann and K.-H. Spatschek, Transient plasma photonic crystals for high-power lasers, *Physical review letters* **116**, 225002 (2016).
- [32] M. Faraday, On the magnetization of light and the illumination of magnetic lines of force, *Philosophical Transactions of the Royal Society of London* **136**, 1 (1846).
- [33] L. Allen, M. W. Beijersbergen, R. J. C. Spreeuw, and J. P. Woerdman, Orbital angular momentum of light and the transformation of laguerre-gaussian laser modes, *Physical Review A* **45**, 8185 (1992).
- [34] M. Harwit, Photon orbital angular momentum in astrophysics, *The Astrophysical Journal* **597**, 1266 (2003).
- [35] G. C. G. Berkhout and M. W. Beijersbergen, Method for probing the orbital angular momentum of optical vortices in electromagnetic waves from astronomical objects, *Physical Review Letters* **101**, 100801 (2008).
- [36] F. Tamburini, B. Thidé, G. Molina-Terriza, and G. Anzolin, Twisting of light around rotating black holes, *Nature Physics* **7**, 195 (2011).
- [37] F. Tamburini, B. Thidé, and M. Della Valle, Measurement of the spin of the M87 black hole from its observed twisted light, *Monthly Notices of the Royal Astronomical Society: Letters* **492**, L2 <https://academic.oup.com/mnrasl/article-pdf/492/1/L22/31505560/>
- [38] F. Tamburini, F. Feleppa, I. Licata, and B. Thidé, Kerr-spacetime geometric optics for vortex beams, *Phys. Rev. A* **104**, 013718 (2021).
- [39] M. Yamada, R. Kulsrud, and H. Ji, Magnetic reconnection, *Rev. Mod. Phys.* **82**, 603 (2010).
- [40] F. F. Chen, *Introduction to plasma physics* (Springer Science & Business Media, 2012).
- [41] S. Weng, Q. Zhao, Z. Sheng, W. Yu, S. Luan, M. Chen, L. Yu, M. Murakami, W. B. Mori, and J. Zhang, Extreme case of faraday effect: magnetic splitting of ultrashort laser pulses in plasmas, *Optica* **4**, 1086 (2017).
- [42] J. Derouillat, A. Beck, F. Pérez, T. Vinci, M. Chiaramello, A. Grassi, M. Flé, G. Bouchard, I. Plotnikov, N. Aunai, J. Dargent, C. Riconda, and M. Grech, Smilei : A collaborative, open-source, multi-purpose particle-in-cell code for plasma simulation, *Computer Physics Communications* **222**, 351 (2018).
- [43] J. W. Goodman, *Introduction to Fourier Optics* (Roberts, 2005).
- [44] E. G. Harris, On a plasma sheath separating regions of oppositely directed magnetic field, *Il Nuovo Cimento* (1955-1965) **23**, 115 (1962).
- [45] Y.-H. Liu, T. C. Li, M. Hesse, W. J. Sun, J. Liu, J. Burch, J. A. Slavin, and K. Huang, Three-dimensional magnetic reconnection with a spatially confined x-line extent: Implications for dipolarizing flux bundles and the dawn-dusk asymmetry, *Journal of Geophysical Research: Space Physics* **124**, 2819 (2019).
- [46] K. Huang, Y.-H. Liu, Q. Lu, and M. Hesse, Scaling of magnetic reconnection with a limited x-line extent, *Geophysical Research Letters* **47**, e2020GL088147 (2020).
- [47] P. A. Cassak, Y.-H. Liu, and M. Shay, A review of the 0.1 reconnection rate problem, *Journal of Plasma Physics* **83**, 715830501 (2017).
- [48] J. Zhong, Y. Li, X. Wang, J. Wang, Q. Dong, C. Xiao, S. Wang, X. Liu, L. Zhang, L. An, F. Wang, J. Zhu, Y. Gu, X. He, G. Zhao, and J. Zhang, Modelling loop-top x-ray source and reconnection outflows in solar flares with intense lasers, *Nature Physics* **6**, 984 (2010).
- [49] D. D. Ryutov, R. P. Drake, and B. A. Remington, Criteria for scaled laboratory simulations of astrophysical MHD phenomena, *The Astrophysical Journal Supplement Series* **127**, 465 (2000).
- [50] L. Torner, J. P. Torres, and S. Carrasco, Digital spiral imaging, *Opt. Express* **13**, 873 (2005).